DØ Note 5414-CONF

Measurement of the $p\bar{p} \to W{+}c$-jet fraction

The D0 Collaboration

(Dated: July 24, 2007)

We present the first measurement of the fraction of W+jets events produced with a net charm quantum number of ± 1, denoted $W{+}c$-jet, in $p\bar{p}$ collisions at $\sqrt{s} = 1.96$ TeV using the D0 detector at the Fermilab Tevatron. The W+jets sample is selected from lepton+jets final states using approximately 1 fb^{-1} of integrated luminosity. The $W{+}c$-jet events are selected by requiring a jet containing a muon in association with a reconstructed W boson and exploiting the charge correlation between this muon and W-decay lepton to perform a nearly model-independent background subtraction. We observe a significant excess of events over background expectations with the characteristics of $W{+}c$-jet, and measure the $W{+}c$-jet fraction in W+jets for jet $p_T > 20$ GeV/c to be 0.071 ± 0.017, in agreement with theoretical predictions.

Preliminary Results for Summer 2007 Conferences

I. INTRODUCTION

In hadron-hadron collisions, the $W/Z+b$- or c-quark hadron jet final state is the signature of many new physics processes; however, only a few measurements [1–3] of the standard model (SM) cross sections for these processes exist, and none involve charm-quark final states. Charm quark production in association with a W boson can be a significant background, for example to $t\bar{t}$ and SM Higgs production, and to supersymmetric top (stop) production when the stop quark's mass limits its possible decays to a charm quark and a neutralino, $\tilde{t} \to \tilde{\chi}_1^0 c$. Moreover, as the Cabibbo-Kobayashi-Maskawa (CKM) matrix element $|V_{cd}|^2$ suppresses the expected leading order d-quark-gluon fusion production mechanism, Wc production provides direct sensitivity to the s-quark parton distribution function (PDF) $s\left(x, Q^2\right)$ in the proton[4]. The s-quark PDF has only been directly measured up to now at fixed-target neutrino-nucleon deep inelastic scattering experiments using relatively low momentum transfer Q^2 probes of the order of 10^{0-2} GeV$^2/c^2$ [5–11]. A probe of this PDF at hadron collider experiments tests the universality of $s\left(x, Q^2\right)$ and its QCD evolution up to scales of order 10^4 GeV$^2/c^2$. The strange quark PDF is dominant for both SM (*e.g.*, $p\bar{p}/pp \to sg \to W^- + c$) and possible new physics processes (*e.g.*, $p\bar{p}/pp \to s\bar{c} \to H^-$) [12] at both the Tevatron and the LHC collider.

In this note, we present a measurement of the cross section ratio $\sigma\left(p\bar{p} \to W + c - jet\right)/\sigma\left(p\bar{p} \to W + jets\right)$, where W+c-jet denotes a W-boson plus jets final state in which the jets have a net charm quantum number $C = \pm 1$, and W+jets denotes any W-boson final state with at least one jet. Many experimental and theoretical uncertainties cancel in this ratio. The measurement utilizes approximately 1 fb^{-1} of $p\bar{p}$ collision data at center-of-mass energy $\sqrt{s} = 1.96$ TeV collected with the D0 detector at the Fermilab Tevatron collider. W-bosons are identified through their leptonic decays, $W \to \ell\nu$, where $\ell = e, \mu$, or τ with $\tau \to e\bar{\nu}_e\nu_\tau$ or $\mu\bar{\nu}_\mu\nu_\tau$. The muon or electron transverse momentum p_T must satisfy $p_T > 20$ GeV$/c$, and the presence of a neutrino is inferred by the requirement that the missing transverse energy $\not\!\!E_T$ satisfies $\not\!\!E_T >$20 GeV. Jets are defined using the iterative seed-based cone algorithm including midpoints with the cone radius $\mathcal{R}_{cone} = 0.5$ [13]. The charm jet's transverse momentum p_T is restricted to $p_T > 20$ GeV$/c$ and its pseudorapidity η to $|\eta| < 2.5$, where $\eta = -\ln\tan(\theta/2)$, with θ the polar angle with respect to the proton beam direction. The key feature for this analysis is the identification of a muon in the event contained within the charm jet candidate (a "μ-tagged jet") and the correlation of that muon's electric charge with that of the W-boson's decay lepton. Events with the jet muon's charge opposite or the same as that of the W-boson are denoted as "OS" or "SS" events, respectively. In the W+c-jet process, the c quark decays into a muon carrying an opposite-sign charge compared to that carried by the W boson, and the number of OS and SS events, N_{OS} and N_{SS}, respectively, satisfy $N_{OS} \gg N_{SS}$ for a W+c-jet sample. The N_{SS} in W+c-jet sample can be non-zero, because a jet initiated with c quark has small probability to contain a muon from the decay of particles other than leading charm. Other vector boson+jets physics processes (W+g, W+$c\bar{c}$, W+$b\bar{b}$, Z+jets) can produce muons contained within a final state, but the jet muon's charge is uncorrelated with that of the boson, hence $N_{OS} = N_{SS}$ for these sources. Processes with light-quark (u, d or s) initiated jets recoiling against the W can produce charge-correlated jets owing to leading particle effects in conjunction to $\pi \to \mu$ or $K \to \mu$ decay, but this correlation is small ($\approx 15\%$). Other final states that can produce charge-correlated jets, $t\bar{t}/t\bar{b}$ and $W + b$, are suppressed by small cross sections and the tiny CKM matrix element $|V_{ub}|^2$, respectively. Backgrounds from WW, WZ and ZZ have been found to be negligible. These considerations allow us to measure the W+c-jet production rate from OS events with the backgrounds determined *in situ* from SS events, up to small weakly model-dependent theory corrections.

II. THE D0 DETECTOR

The D0 detector [14] is a multi-purpose device built to investigate $p\bar{p}$ collisions at high energies. The innermost silicon microstrip detectors (SMT) followed by the scintillating fiber tracking detector (CFT), covering the η range up to ≈ 3.0, located inside the 2 T superconducting solenoid, are used for tracking and vertexing. The liquid-argon and uranium calorimeter, a finely segmented detector in the transverse and the longitudinal directions, is used as a primary tool to construct the electron, the jets and the missing transverse energy of neutrinos. It is housed in three cryostats, one central calorimeter (CC) in the region $|\eta| < 1.1$ and two end caps (EC) extending the coverage to $|\eta| \approx 4.0$. The outermost subsystem of D0 detector is the muon spectrometer, consisting of three layers of muon tracking subdetectors and scintillation trigger counters, is used to construct the muon up to $|\eta| \approx 2.0$. One of them (layer A) is situated before the 1.8 T magnetized toroid and the other two (B and C layers) are outside enclosing the detector.

TABLE I: Summary of quantities used in W+c-jet cross section ratio.

jet p_T[GeV/c]	20-30	30-45	45-200	20-200
$< p_T >$[GeV/c]	23.9	35.1	62.3	34.6
N^e_{Wj}	38556	26347	24539	89442
N^e_{OS}	87	79	88	254
N^e_{SS}	49	45	72	166
f^e_c	1.177±0.013	1.159±0.015	1.117±0.028	1.145±0.007
ϵ^e_c	0.0113±0.0015	0.0125±0.0011	0.0125±0.0020	0.0124±0.0012
$\frac{\sigma[W(\to e\nu)+c]}{\sigma[W(\to e\nu)+jets]}$	0.070±0.031	0.084±0.038	0.026±0.046	0.060±0.021
N^μ_{Wj}	27828	17594	13446	58868
N^μ_{OS}	76	64	63	203
N^μ_{SS}	28	38	56	122
f^μ_c	1.195±0.025	1.174±0.015	1.121±0.035	1.143±0.007
ϵ^μ_c	0.0110±0.0011	0.0122±0.0013	0.0148±0.0018	0.0122±0.0012
$\frac{\sigma[W(\to \mu\nu)+c]}{\sigma[W(\to \mu\nu)+jets]}$	0.145±0.040	0.095±0.054	0.001±0.062	0.093±0.029

III. EVENT SELECTION

A. Trigger

Candidate events in the electron (muon) decay channel of the W-boson are required to pass at least one of the single electron (muon) three-level triggers (L1, L2 and L3) used in each data taking period. The single electron triggers at L1 require to have an electromagnetic (EM) object to deposit an energy of at least 10 GeV in the EM section of the calorimeter. At L2, a relatively higher transverse energy requirement is imposed for a subset of data. At L3, these triggers require a certain fraction of the EM energy deposited in the EM section and impose some matching requirements to the shower shape of deposited energy with that of an electron. The single muon triggers at L1 impose hits in the muon scintillators. Some of the triggers also require spatially matched hits in the muon tracking detectors. At L2, a good quality muon object reconstructed from muon track segments is required with a minimum p_T that varies for different triggers. At L3, certain triggers require a track reconstructed in the inner tracking system with $p_T > 10$ GeV/c.

B. Reconstructed objects selection

To select $W \to e\nu$ candidates, we require an isolated high-p_T electron similar to that described in Ref. [15]. We require that a cluster of energy be found that is consistent with the presence of an electron in the calorimeter. The cluster must: have 90% of the energy contained in the electromagnetic part of the calorimeter; have a reconstructed track from the inner tracking system pointing to it; be isolated from other clusters in that the fraction of the energy deposited in a halo cone ($0.2 < \mathcal{R} < 0.4$) around the EM cluster should be less than 15% of the energy in the cone of radius $\mathcal{R}$= 0.2; have a longitudinal and transverse energy deposition profile consistent with that expected for an electron; pass a likelihood discriminant that combines tracker and calorimeter information with the expected distributions for electrons and jet backgrounds. The electron track should originate within 5 cm of the $p\bar{p}$ interaction point along the z-axis of the detector; and the interaction point must lie within $|z| < 60$ cm of the nominal beam crossing position.

$W \to \mu\nu$ candidates are selected by following the criteria similar to that described in Ref. [15]. We require that a muon candidate be found in the muon spectrometer with a track matched to one found in the central tracker. Cosmic ray events are rejected by requiring the central track to pass within 0.02 (0.2) cm of the beam crossing point in the transverse plane if the track is reconstructed with(without) SMT hits, to originate within 3 cm of the interaction point, and by using scintillator hits timing information in the muon spectrometer. Isolated muons from semileptonic decays of heavy flavor quarks in QCD multi-jet events are suppressed by requiring the W candidate muon track to be separated with respect to the axis formed by any jet found in event by the criterion $\Delta\ \mathcal{R}(\mu, jet) > 0.5$.

For the final event selection in both electron and muon channel, each event must: have a missing transverse energy $\not{E}_T$ of at least 20 GeV, have a transverse mass m_T computed from the isolated lepton p_T and the $\not{E}_T$ in the range $40 - 120$ GeV/c^2, and have at least one jet with $p_T > 20$ GeV/c. Upon application of all selection criteria there are $N^e_{Wj} = 89442$ and $N^\mu_{Wj} = 58868$ W+jets candidates in the electron and muon channels, respectively.

C. W+jets background

Backgrounds from mis-identified W-bosons arise from photons (γ's) or jets that are misidentified as electrons in the electron channel, with a fractional contamination $f_B^e = (3.3 \pm 0.5)\%$, and from $Z \to \mu^+\mu^- + jets$ events where one of the Z decay muons is not reconstructed in the muon channel, with fractional contamination $f_B^\mu = (4.7 \pm 0.6)\%$. The electron channel background is determined directly from the data by measuring the jet-to-electron misidentification probability using a large sample of QCD two jet events with some contribution of γ+jet events. The $Z \to \mu^+\mu^-$ background is estimated using Monte Carlo simulations of vector boson +jets production produced with ALPGEN [16] using the PDF set CTEQ6L [17], the PYTHIA [18] generator for the parton fragmentation and hadronization with the MLM prescription [19] to avoid an over-counting of final state jets, and the EVTGEN [20] to decay the heavy hadrons; a GEANT [21] based program to simulate the effects of detector response; and the same reconstruction software as used for data. The muon channel background's uncertainties are associated with systematic effects in the vector boson +jets cross section model and are estimated by varying parameters in ALPGEN.

D. W+c-jet selection

To isolate a sample of W+c-jet event candidates from the W+jets sample, we select events with a μ-tagged jet. This jet must have $p_T > 20$ GeV/c and contain a reconstructed muon with transverse momentum $p_T > 4$ GeV/c and $|\eta| < 2.0$ that lies within a cone of $\Delta\mathcal{R}(jet, \mu) < 0.5$ with respect to the jet axis. The jet muon must be detected in both of the outer two layers of the muon spectrometer, and its muon spectrometer track segment must be matched to a reconstructed track in the central tracker. In the $W \to \mu\nu$ channel, the requirement for the two muons in the final state leads to small contamination from $Z \to \mu^+\mu^-$+jets events in which one of the muons from the Z decay is found inside a jet cone. This contribution to μ-tagged jets is suppressed by rejecting events in which the dimuon invariant mass exceeds 70 GeV/c^2. Application of all selection criteria yields $N_{OS}^e = 254$ and $N_{SS}^e = 166$ events in the $W \to e\nu$ channel, and $N_{OS}^\mu = 203$ and $N_{SS}^\mu = 122$ events in the $W \to \mu\nu$ channel.

E. Relative efficiency of W+c-jet selection

We use the ALPGEN-PYTHIA-EVTGEN-GEANT simulation package and a large D0 data sample to calculate the relative acceptance×efficiencies $\epsilon_c^\ell\,(\ell = e, \mu)$ in each W decay channel of finding a reconstructed jet muon that satisfies the selection criteria in a jet initiated by a c-quark to that of simply reconstructing a W-boson with at least one jet in the final state. This acceptance incorporates effects of charm quark to hadron fragmentation and charmed hadron semi-muonic decay. The efficiency accounts for muon identification and track reconstruction effects. Charm quark fragmentation and charm hadron decay are well known from previous measurements and contribute negligibly to the acceptance uncertainty. We use a large sample of $J/\psi \to \mu^+\mu^-$ events collected at D0 to correct the efficiency, $(58.7 \pm 0.4)\%$, computed from the Monte Carlo simulation by a factor of 0.89 ± 0.04. This correction is found to be independent of the jet p_T. For the electron and muon channels the total acceptance×efficiencies are found to be $(1.24 \pm 0.12)\%$ and $(1.22 \pm 0.12)\%$, respectively. As expected, the μ-tagged jet reconstruction efficiencies in the two W-decay modes differ only by the small effect of the dimuon invariant mass condition applied in the $W \to \mu\nu$ mode.

IV. W+c-JET / W+JETS CROSS-SECTION RATIO

We then proceed to extract the relative W+c-jet cross section from the expression

$$\frac{\sigma\left[W(\to \ell\nu) + c - jet\right]}{\sigma\left[W(\to \ell\nu) + jets\right]} = \frac{N_{OS}^\ell - f_c^\ell N_{SS}^\ell}{(1 - f_B^\ell) N_{Wj}^\ell \times \epsilon_c^\ell},$$

which requires one further small correction, f_c^ℓ, that accounts for the small correlation between the tag muon and W boson charge that arises from the decay of the most energetic pion or kaon having an enhanced probability of containing the highest p_T quark recoiling against W-boson generated at the hard scatter vertex that fragments into jet.

We determine f_c^ℓ from fully simulated ALPGEN-PYTHIA-EVTGEN-GEANT W+jet events as the ratio of the predicted number of OS μ-tagged jets to the predicted number of events containing the SS μ-tagged jets in the background sample that pass the same selection criteria as defined for the data sample. Processes considered include W+u, d, s, W+g, W+$c\bar{c}$, W+$b\bar{b}$, and W+c-jet, where the c quark does not decay muonically in the last case. Studies show

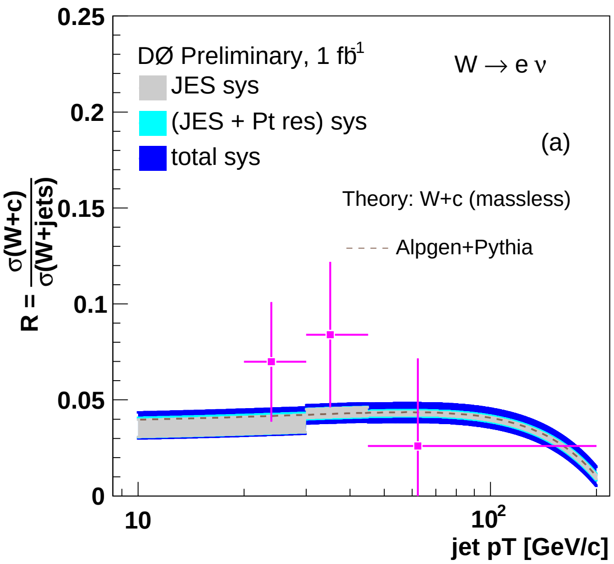

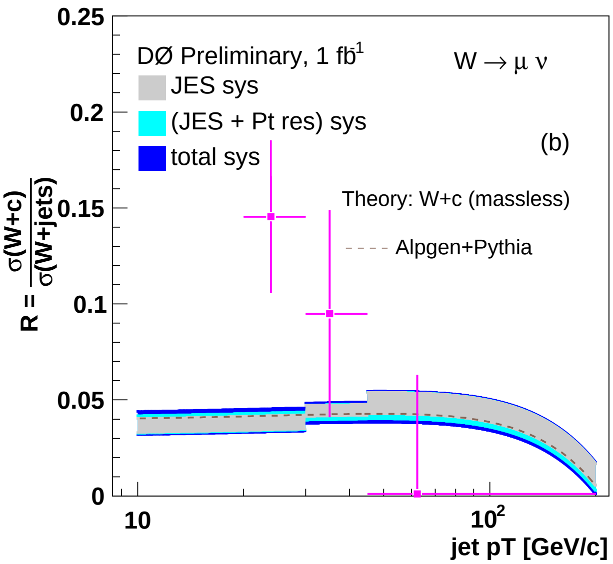

FIG. 1: Measured ratio $\frac{\sigma(W+c-jet)}{\sigma(W+jets)}$ for jet $p_T > 20$ GeV/c and $|\eta| < 2.5$. (a) Electron decay channel, (b) muon decay channel.

that f_c^ℓ can be parameterized in terms of jet p_T as $f_c^\ell = a_\ell + b_\ell \times p_T$, with $a_e = 1.214 \pm 0.012$, $a_\mu = 1.241 \pm 0.023$, $b_e = -0.0016 \pm 0.0002$, and $b_\mu = -0.0019 \pm 0.0004$; f_c^ℓ decreases with increasing jet p_T because the sub-process $q\bar{q} \to Wg$ becomes dominant over $qg \to Wq'$ at high jet p_T. Systematic uncertainties on f_c^ℓ arise mainly from the cross section and jet fragmentation models. To first order, the f_c^ℓ are independent of the absolute charged multiplicity per jet and the W+light-jets cross section; it depends instead on the $K^\pm/\pi^\pm$ ratio per jet and the relative cross section for W plus heavy quark jet final states compared to W+light-jets. We attribute a 6% uncertainty on the weighted $\pi^\pm$ multiplicity based on a comparison of the difference between tracking efficiency in data and simulation, and a 20% uncertainty on the $K^\pm/\pi^\pm$ ratio based on comparing K_S^0 production in data to Monte Carlo simulation. We assign uncertainties in the ALPGEN cross-sections of 50% for $W+b\bar{b}$, $W+c\bar{c}$, and $W+c$-jet, relative to W+light-jets. The uncertainty on $W+b\bar{b}$ and $W+c\bar{c}$ cross-section is associated with the relative scale factor 1.50 ± 0.45 which is suggested for better agreement between data and prediction for inclusive W+jets [22]. A change of the $W+c$-jet cross-section by $\pm 100\%$ does not lead to a significant effect in f_c^ℓ. The overall systematic uncertainty is found to 1.2% for f_c^e and 0.6% for f_c^μ, with the relative cross section contributions dominant. Adding a 0.6% uncertainty in each channel due to Monte Carlo statistics, we find that, averaged over all $p_T > 20$ GeV/c, $f_c^e = 1.145 \pm 0.015$ and $f_c^\mu = 1.143 \pm 0.009$.

A. Systematic uncertainties

Table I summarizes the cross section ratio measurements and their uncertainties for the electron and the muon channels for all jet $p_T > 20$ GeV/c and jet $|\eta| < 2.5$, and for three jet p_T bins. The ratio measurements benefit from the large cancellation of several uncertainties, notably the integrated luminosity [23], lepton detection efficiency, and jet energy scale (JES). Remaining absolute systematic uncertainties on the measurement estimated from the Monte Carlo simulation are given in the Table II. These uncertainties are mainly from residual effects of JES, jet energy resolution (JER), the efficiency of c-jet tagging, and the $W+c$-jet background correction factor f_c^ℓ.

V. RESULT

Figures 1(a) and (b) compare the data with model predictions using leading order QCD augmented by ALPGEN and PYTHIA for the electron and the muon channels respectively. Due to relatively small contribution of $W+b\bar{b}$ and $W+c\bar{c}$ into inclusive W+jets, the $W+c$-jet rate has $\approx 1\%$ sensitivity to their cross-sections. The grey band

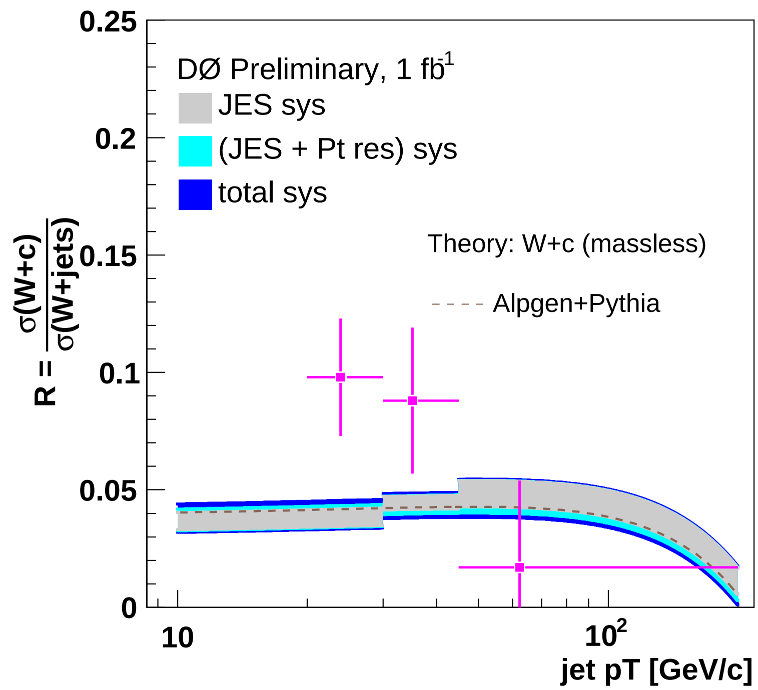

FIG. 2: Measured ratio $\frac{\sigma(W+c-jet)}{\sigma(W+jets)}$ for jet $p_T > 20$ GeV/c and $|\eta| < 2.5$. The results from the electron and muon decay channels are combined.

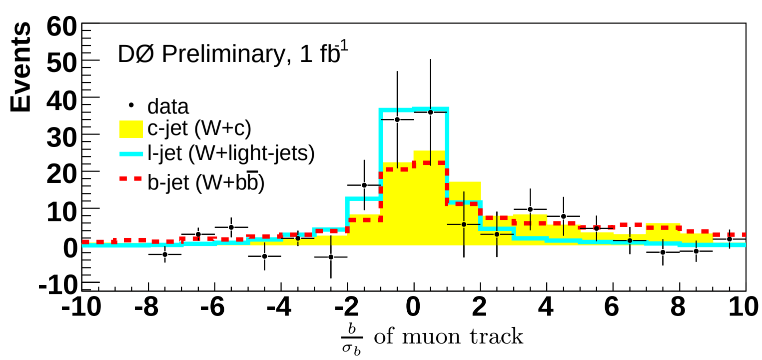

FIG. 3: Comparison of the *signed* significance in impact parameter distribution of the jet muon track with respect to the interaction point in data in the combined electron and muon channels with the simulation. The background is subtracted based on SS events using the procedure described in the text.

shown around the theory curve is the systematic uncertainty on the W+c-jet fraction estimated from simulation due to JES only, and the blue outer band is the combined systematic uncertainty due to the JES, the jet's relative p_T resolution in data and simulation, the background correction factor f_c^l and the relative acceptance × efficiency ϵ_c^l. The intermediate cyan band shows only the systematic uncertainty due to JES and jet's relative p_T resolution. Since the two measurements are consistent with one another, and the uncertainties on the measurement are dominantly statistical, they are combined to yield the differential W+c-jet fraction as shown in Fig. 2. In the combined plot the systematic errors are assumed to be fully correlated. The measured W+c-jet fractions integrated over $p_T > 20$ GeV/c are $\sigma\left[W(\rightarrow e\nu) + c - jet\right]/\sigma\left[W(\rightarrow e\nu) + jets\right] = 0.060 \pm 0.021$(statistical) $\pm^{0.005}_{0.007}$(systematic) and $\sigma\left[W(\rightarrow \mu\nu) + c - jet\right]/\sigma\left[W(\rightarrow \mu\nu) + jets\right] = 0.093 \pm 0.029$(statistical) ± 0.005(systematic). Combining the two measurements yield $\sigma\left[W + c - jet\right]/\sigma\left[W + jets\right] = 0.071 \pm 0.017$, with a significant excess of OS events relative to SS events which we attribute to W+c-jet production. The W+c-jet fraction predicted by ALPGEN and PYTHIA is

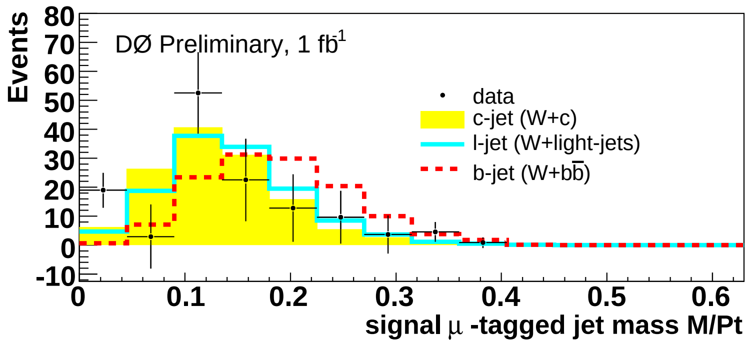

FIG. 4: Comparison of the jet mass divided by the jet p_T distribution in data and simulation in shape.

TABLE II: Systematic uncertainties on the measurement in the $W \to e\nu$ and the $W \to \mu\nu$ channels.

		e-channel			μ-channel		common
p_T	JES	JER	f_c^e	JES	JER	f_c^μ	ϵ_c^l
20-30	$\pm^{0}_{0.009}$	$\pm^{0.002}_{0.003}$	± 0.002	$\pm^{0}_{0.007}$	$\pm^{0.002}_{0.003}$	± 0.001	± 0.004
30-45	$\pm^{0.003}_{0.002}$	$\pm^{0.002}_{0.003}$	± 0.002	$\pm^{0.005}_{0.001}$	$\pm^{0.002}_{0.003}$	± 0.001	± 0.004
45-200	$\pm^{0.001}_{0.001}$	$\pm^{0.002}_{0.003}$	± 0.003	$\pm^{0.011}_{0}$	$\pm^{0.002}_{0.003}$	± 0.001	± 0.003
20-200	$\pm^{0}_{0.004}$	$\pm^{0.002}_{0.003}$	± 0.002	$\pm^{0.002}_{0.001}$	$\pm^{0.002}_{0.003}$	± 0.001	± 0.004

0.040±0.003, where the quoted uncertainty is due to the PDFs.

As a test of the W+c-jet signal hypothesis, Fig. 3 compares data to ALPGEN/PYTHIA expectations of heavy flavor and light-jet shapes in the background-subtracted distribution of the signed impact parameter significance b/σ_b for the jet muon, where b is the projected distance of closest approach of the jet muon to the event interaction point in the transverse plane and σ_b is the estimated uncertainty on b. In Fig. 4, the distribution of the invariant mass of well reconstructed tracks in the jet cone divided by the jet p_T is shown to compare the background-subtracted distribution in data with b-jet, c-jet and light-parton jet templates. The b-jet distribution of b/σ_b has relatively (compared to central peak) large positive tail due to longer life time, and the data show satisfactory agreement with expectations for W+c-jet production. The asymmetry present in b/σ_b distribution is consistent with the underlying ansatz wherein light quark jet contributions are subtracted out. At the same time, the jet mass (M) to p_T ratio distribution shows that the data favors the c-jet template over that for b-jet. Due to smaller masses of light and c partons, the light-jet and c-jet distributions peak at the lower values of M/p_T ratio compared to the b-jet. We emphasize that Figs. 3 and 4 represent only consistency checks for the W+c-jet interpretation; these distributions cannot conclusively separate W+c-jet from $W + b\bar{b}$ or, especially, $W + c\bar{c}$.

VI. CONCLUSION

In conclusion, we have performed a first measurement of the W+c-jet/W+jets cross section ratio at a hadron collider using both electron and muon decay modes of the W and establishing a correlation between the charge of muon-tagged jets with that of the W. We find our measurement to be consistent with LO perturbative QCD predictions of the W+c-jet production rate, and with an s-quark PDF evolved from Q^2 scales two orders of magnitude below that of the Tevatron. This measurement provides direct experimental evidence of the underlying partonic process $qg \to q'W$ that should dominate W production at the LHC collider.

Acknowledgments

We thank the staffs at Fermilab and collaborating institutions, and acknowledge support from the DOE and NSF (USA); CEA and CNRS/IN2P3 (France); FASI, Rosatom and RFBR (Russia); CAPES, CNPq, FAPERJ, FAPESP and FUNDUNESP (Brazil); DAE and DST (India); Colciencias (Colombia); CONACyT (Mexico); KRF and KOSEF (Korea); CONICET and UBACyT (Argentina); FOM (The Netherlands); Science and Technology Facilities

Council (United Kingdom); MSMT and GACR (Czech Republic); CRC Program, CFI, NSERC and WestGrid Project (Canada); BMBF and DFG (Germany); SFI (Ireland); The Swedish Research Council (Sweden); CAS and CNSF (China); Alexander von Humboldt Foundation; and the Marie Curie Program.

[1] (CDF collaboration) *Measurement of the b-jet Cross-Section for* $W^{\pm}+b\bar{b}$ *Production* Conference Note 8410.
[2] A. Abulencia *et al.* (CDF Collaboration) Phys. Rev. **D74**, 032008 (2006).
[3] V.M. Abazov *et al.* (D0 collaboration) Phys. Rev. Lett. **94**, 161801 (2005).
[4] U. Baur, F. Halzen, S. Keller, Michelangelo L. Mangano, K. Riesselmann, Phys. Lett. **B318**:544-548 (1993).
[5] D. A. Mason, *Measurement of the Strange-Antistrange Asymmetry at NLO in QCD from NuTeV Dimuon Data*, FERMILAB-THESIS-2006-01.
[6] M. Goncharov *et al.* (NuTeV collaboration), Phys. Rev. **D64**, 112006 (2001) [hep-ex/0102049].
[7] S. A. Rabinowitz *et al.* (CCFR collaboration), Phys. Rev. Lett. **70**, 134 (1993).
[8] A. O. Bazarko *et al.* (CCFR collaboration), Z. Phys. **C65**, 189 (1995).
[9] P. Vilain *et al.* (Charm II Collaboration), Eur. Phys. J. **C11**: 19-34 (1999).
[10] H. Abramowicz *et al.* (CDHS collaboration), Z. Phys. **C15**, 19 (1982b).
[11] M. Holder, *et al.* (CDHS collaboration), Phys. Lett. **B69**, 377 (1977a).
[12] H. L. Lai *et al.*, *The Strange Parton Distribution of the Nucleon: Global Analysis and Applications*, arXiv:hep-ph/0702268v2, (April 9, 2007).
[13] G.C. Blazey *et al.*, in *Proceedings of the Workshop: QCD and Weak Boson Physics in Run II,* edited by U. Baur, R.K. Ellis, and D. Zeppenfeld, Fermilab-Pub-00/297 (2000).
[14] V.M. Abazov *et al.* (D0 Collaboration), Nucl. Instrum. Methods Phys. Res. **A565**, 463 (2006).
[15] V.M. Abazov *et al.* (D0 Collaboration), Phys. Rev. **D74**, 092005 (2006).
[16] M.L. Mangano *et al.*, CERN-TH/2002-129.
[17] J. Pumplin *et al.*, JHEP **0207** 012 (2002) and D. Stump *et al.*, JHEP **0310** 046 (2003).
[18] T. Sjöstrand *et al.*, Comput. Phys. Commun. **135**, 238 (2001).
[19] S. Hoeche *et al.*, *Proceedings of the "HERA and the LHC" workshop, CERN/DESY 2004/2005*, arXiv:hep-ph/0602031v1.
[20] D.J Lange, Nucl. Instrum. Methods Phys. Res., Sect. **A462**, 152 (2001).
[21] R. Brun and F. Carminati, CERN Program Library Long Writeup W5013, (1993) (unpublished).
[22] V.M. Abazov *et al.* (D0 Collaboration), Phys. Rev. Lett. **98**, 181902 (2007).
[23] T. Andeen *et al.*, FERMILAB-TM-2365-E (2006).